Influence of rotary forging and post-deformation annealing on mechanical and functional properties of titanium nickelide

V. A. Andreev · R. D. Karelin · V. S. Komarov · V. V. Cherkasov · N. A. Dormidontov · N. V. Laisheva · V. S. Yusupov

Received: 12 October 2023 / Revised: 27 October 2023 / Accepted: 15 November 2023 / Published online: 4 June 2024

Abstract
This work studies the influence of thermomechanical processing modes, including rotary forging and post-deformation annealing at various temperatures and holding times, on the structure and mechanical properties of titanium nickelide alloy with shape memory effect of near-equiatomic composition. Rotary forging was carried out at a temperature of 450 °C from 12 to 5 mm with a true accumulated strain of $e = 1.8$. Post-deformation annealing was carried out in the temperature range from 450 to 550 °C for 0.5–1 h. The structure of the alloy following rotary forging and post-deformation annealing was studied using transmission electron microscopy. Mechanical properties were studied by tensile testing. Functional properties were determined using the thermomechanical method under bending deformation. It was found that rotary forging leads to the formation of an ultrafine-grained structure in the TiNi alloy with a high density of defects and sizes of structural elements in the range of 100–250 nm. Post-deformation annealing at 450 °C results in no increase in the average size of structural elements. At the same time, the dislocation density visually decreases. After rotary forging, the TiNi SMA rod is characterized by strong strain hardening compared to the state after reference treatment (annealing at 750 °C, 30 min, cooling in water), since a sharp increase in strength characteristics is observed. Post-deformation annealing leads to a slight decrease in strain hardening, and with an increase in the post-deformation annealing temperature and holding time, a more noticeable decrease in strength characteristics occurs. After inducing 7% strain, there is no residual strain following all considered rotary forging and post-deformation annealing regimes, with the exception of annealing at a temperature of 550 °C for 1 h, which is a confirmation of a significant increase in the shape recovery characteristics as a result of the applied processing modes.

Keywords Shape memory alloy · TiNi · Thermomechanical treatment · Rotary forging · Post-deformation annealing · Mechanical properties

Introduction

Shape-memory alloys (SMA) based on titanium nickelide (TiNi) are widely used in engineering and medicine as functional materials for the manufacture of various devices, such as clamps and stents for use in cardiovascular surgery, dental arches and retainers for orthodontics, implants for orthopedics, endodontic instruments, functional elements of space antennas, and thermosensitive elements of fire alarm systems [1–10]. Device arrangement

Translated from *Metallurg*, No. 12, pp 87–92, December, 2023. Russian DOI: https://doi.org/10.52351/00260827_2023_12_87

that includes elements with shape memory is constantly becoming more complex due to the need to improve their design, reduce metal consumption, and meet extended requirements for reversible deformation capacity and operating temperature range.

For the manufacture of most devices operating on the basis of the shape memory effect (SME), semi-finished long bars of various grades are used. It is known that the use of thermomechanical processing (TMP), which involves intensive plastic deformation (IPD) at a dynamic polygonization temperature (300–500 °C), leads to the formation of an ultra-fine grain (UFG: submicro- and nanocrystalline) structure, which allows mechanical and functional properties to be improved [11, 12]. Currently, the methods of intensive plastic deformation (such as equal channel angular pressing, high-pressure torsion, deformation in MaxStrain deformation system, and abc pressing) allow a bulk and long UFG structure to be formed only in small experimental samples. However, it is necessary to develop the methods to form a UFG structure in bulk and long blanks under industrial conditions.

Hot rotary forging (HRF) is typically used to manufacture round and long bars. Conventional forging is carried out at high temperatures (800–900 °C), since this significantly simplifies the deformation process, reducing the likelihood of internal stresses and cracks. However, at these temperatures, the processes of recrystallization and growth of structural elements occur, hindering the formation of a UFG structure. Based on literature data and previous experience with deformation methods, it is recommended that the temperature of rotary forging (RF) be less than 500 °C in order to obtain the desired UFG structure [11–14]. The temperature and duration of post-deformation annealing to shape the finished SMA TiNi product, as well as to obtain the required performance characteristics, typically range from 300 to 550 °C and from 0.5 to 5 h, respectively. These parameters can have a noticeable effect on both the temperature range required to recover the shape and the mechanical and functional characteristics of the finished product.

This paper examines the impact of thermomechanical processing modes, including warm rotary forging (WRF) and post-deformation annealing at various temperatures and holding times, on the structure and mechanical properties of a near equiatomic alloy with shape memory based on titanium nickelide.

Materials and methods

Hot-rolled rods with a diameter of 20 mm made of a Ti–50.0 at % Ni alloy were used as the initial blanks. Prior to WRF, blanks measuring 250 mm in length, cut from the obtained rods, were annealed at a temperature of 750 °C for 30 min, followed by cooling in water, which corresponded to the reference treatment (RT).

In addition, prior to RF, the rods were subjected to HRF to the diameter of 12 mm at a temperature of 850 °C and a relative deformation per pass of 10–15%. Subsequently, annealing was carried out at 750 °C for 30 min, followed by quenching in water. Further, the WRF was carried out to the diameter of 5.0 mm at a temperature of 450 °C with a relative degree of deformation per pass of less than or equal to 7% and a true accumulated strain $e = 1.8$. Following the WRF, post-deformation annealing (PDA) was carried out at temperatures of 450, 500, and 550 °C for 1 h and at temperatures of 450 and 500 °C for 30 min.

A JEM-2100 transmission electron microscope (TEM) was used to study the alloy structure following RF at room temperature. The average size of structural elements was estimated using the random linear intercept method on bright-field images, with at least 200 structural units analyzed for each state. The obtained data were subjected to statistical processing in order to determine the confidence interval with a coefficient of determination of 0.99. The mechanical properties were determined by uniaxial tensile tests using an INSTRON 3382 universal testing machine at a deformation rate of 2 mm/min at room temperature. According to the obtained tensile diagrams, the main mechanical properties were determined, including phase yield strength (σ_p)—stress corresponding to the onset of accumulation of reversible deformation as a result of martensite transformation under load with the formation of deformation-induced martensite, dislocation yield strength (σ_y)—stress corresponding to the onset of plastic deformation of the alloy, tensile strength (σ_B), and elongation at break (δ). In addition, functional characteristics, including deformation at yield point ($_r$), tensile stress at

Fig. 1 General view of SMA TiNi sample prior to and following tensile tests

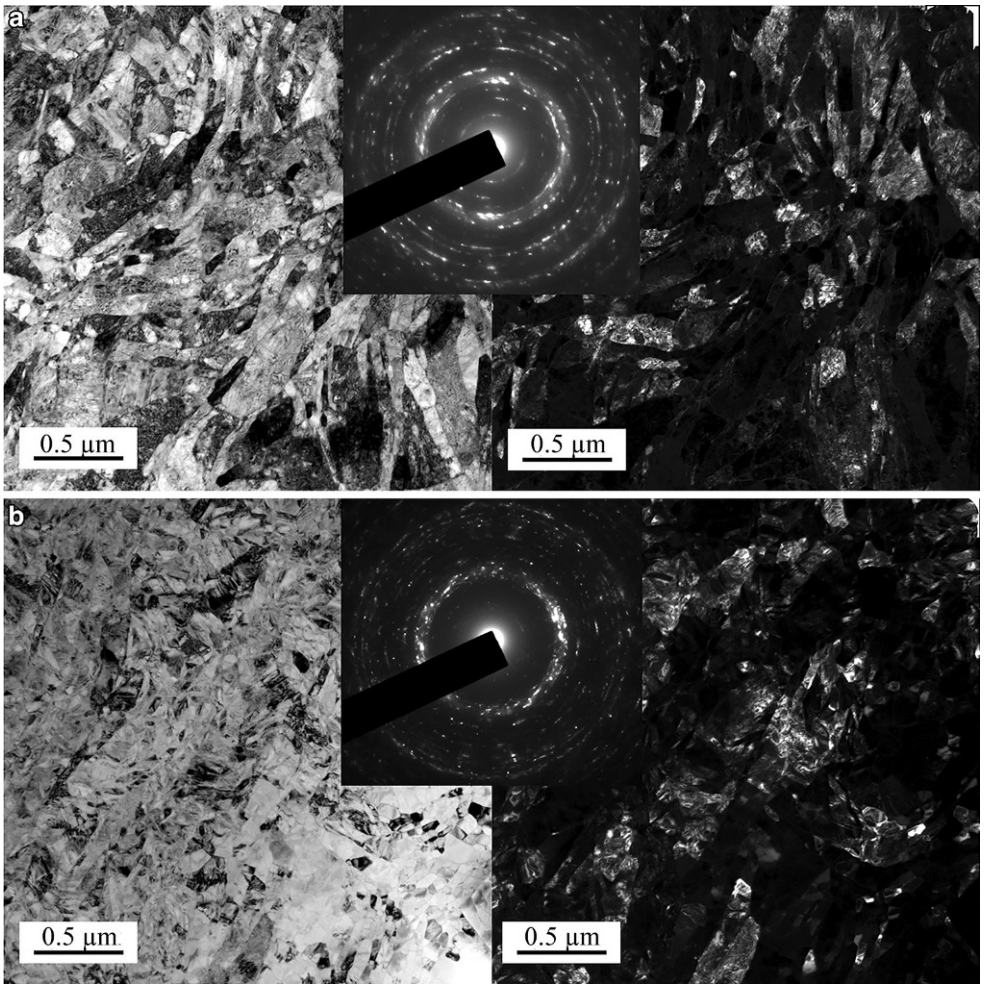

Fig. 2 Structure of SMA TiNi following WRF (**a**) and PDA (**b**) at 450 °C for 1 h. TEM. From left to right: bright-field images, dark-field images, in the center—diffraction patterns

an elongation of 6% (σ_{mps}), and the difference between phase and dislocation yield strength ($\Delta\sigma$) with an instrumental error of ±15 MPa for σ and ±1.4% for δ, were determined. Flat samples having a thickness of 1 mm, a width of 5 mm, and a length of 55.0 mm, with a working part having a width of 2.0 mm and a length of 10.0 mm, were used for mechanical tensile tests. The general view of a sample prior to the tensile test is shown in Fig. 1.

The temperature range for the shape recovery and the maximum completely recoverable strain were estimated using the thermomechanical method for bending deformation of samples with a thickness d around mandrels with a diameter D, which was varied to alter the value of induced strain ε_i from 2.6–3.0 and up to 7.4–7.7%. The test samples were cut into sticks measuring 0.55 × 1.0 × 20 mm. The SME parameters were determined based on the ratio: $\varepsilon = d / (D + d)$. To determine the diameter of the arc, arc templates with different diameters were manufactured. The total induced strain was determined using the expression $\varepsilon_t = d / (D + d)$. Subsequently, following the removal of the load and the recovery of the elastic and superelastic strain, the induced deformation was determined by $\varepsilon_i = \varepsilon_t - \varepsilon_e$. Further, samples were heated to carry out SME, following which the residual

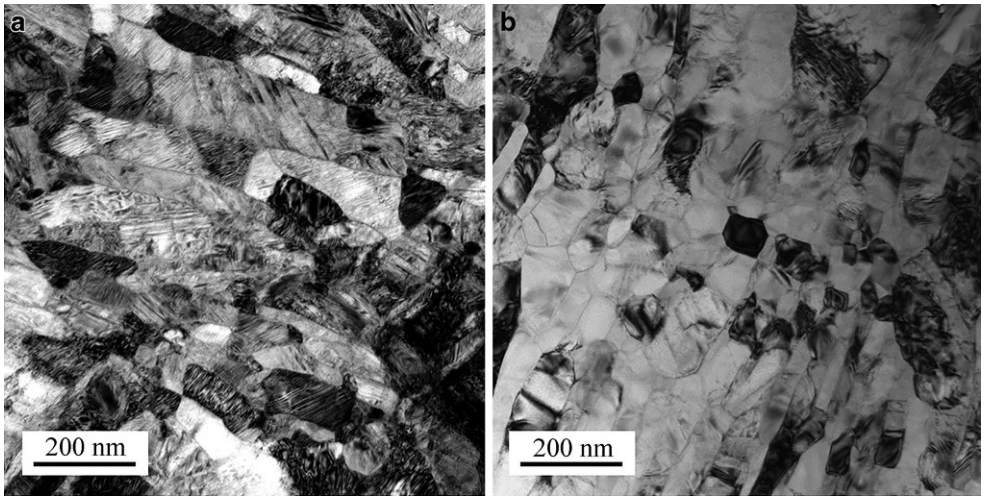

Fig. 3 Bright-field images of a structure following WRF (**a**) and PDA (**b**) at 450 °C for 1 h. *TEM* bright-field images

strain ε_f was determined by comparing the samples with the reference arcs. The maximum value of recoverable strain was determined as $\varepsilon_r = \varepsilon_i - \varepsilon_f$. The shape recovery rate (SRR) was calculated using the following formula: $SRR = \varepsilon_r{}^{max} / \varepsilon_i \cdot 100\%$. The absolute error in determining recoverable strain was ±0.3%.

To determine the temperature range for shape recovery (TRSR), the thermomechanical method (TMM) was used as follows. Following inducing strain (no more than 3.0%), the sample was placed in water. Subsequently, with a gradual increase in water temperature, the starting and finishing temperatures of shape recovery was recorded, which corresponded to the temperature of the starting (A_s) and the finishing (A_f) of reverse martensitic transformation following induced strain.

Results and discussion

Microstructure of SMA TiNi following rotary forging and PDA. Figures 2 and 3 demonstrate the images of the fine microstructure of SMA TiNi samples following WRF and PDA at 450 °C for 1 h obtained by transmission electron microscopy.

A complex structure formed during WRF combined with PDA was identified by analyzing the obtained images. As a result of the WRF, a UFG structure with a high dislocation density (at least 10^{11} cm^{-2} on visual inspection) was formed in the alloy, along with a large number of nanoscale structural elements (grains and subgrains). In the brightfield images of the sample after WRF, mainly equiaxial structural elements are present, characterized by both low and high-angle misorientations. This is confirmed by analysis of dark-field images and diffraction patterns, which show both point and arc reflections. The reflections on diffraction patterns obtained at room temperature mainly correspond to various crystallographic planes of B19′-martensite and *R*-phase. The azimuthal broadening of the reflections is associated with the misorientation of the crystal lattice in these areas, which reaches several degrees. In addition, the individual point reflections from individual grains can be observed. Statistical analysis of the size of structural elements showed that following the WRF, a mixed submicrocrystalline structure was obtained in the alloy, including grains with a diameter of 100 to 250 nm with clusters of subgrains of similar size and high dislocation density. The average size of the structural elements was 138 ± 15 nm. Analysis of the bright-field images of the structure obtained at higher magnification revealed that, following the WRF, deformation bands are present in the structure, where a grain-subgrain structure with high dislocation density is observed. The PDA at a temperature of 450 °C significantly reduces the number of

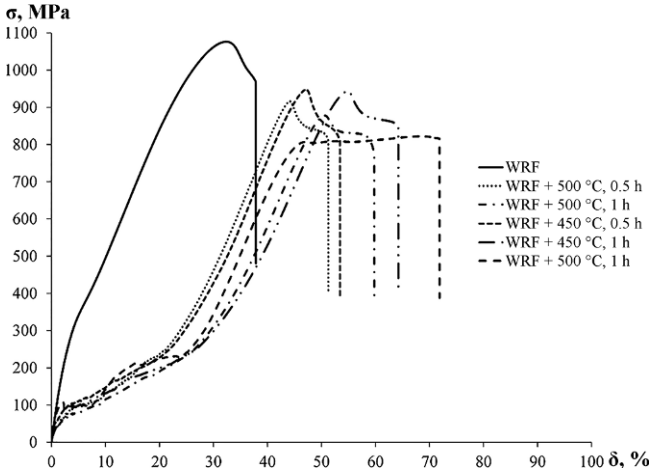

Fig. 4 Typical deformation diagrams of SMA TiNi following WRF and PDA

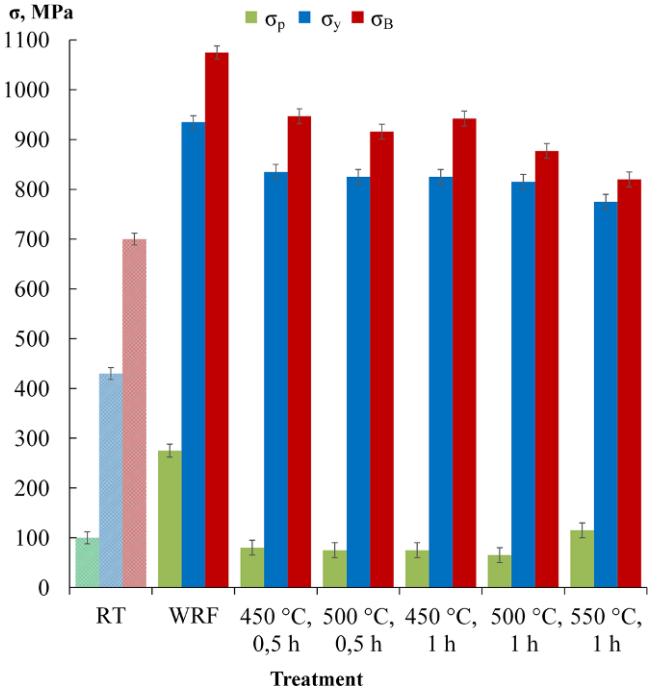

Fig. 5 Variations in strength characteristics of SMA TiNi following WRF and PDA

defects in the structure, which is more homogeneous due to the processes of static polygonization. This is also reflected in the reduction of the azimuthal broadening of the reflections in the diffraction pattern (Fig. 2). The average size of the structural elements remained virtually unchanged following the PDA (136 ± 12 nm).

Results of mechanical tests

Typical tensile diagrams of SMA TiNi samples following WRF and PDA are shown in Fig. 4. The results of the analysis of the obtained diagrams are summarized in Table 1.

Following WRF at 450 °C, the SMA TiNi rod is characterized by high strain hardening compared to the state following CT, since a sharp increase in the strength characteristics, including the phase yield strength, is observed: σ_p increases from 100 to 275 MPa, σ_y—from 430 to 935 MPa, σ_B—from 700 to 1075 MPa. PDA leads to a certain decrease in the strain hardening, reflected in a decrease in tensile strength and an increase in the plasticity of the alloy. The diagram of the main mechanical characteristics as a function of the annealing mode is shown in Fig. 5. With an increase in the PDA temperature and the holding time, the strength characteristics of the TiNi SMA decrease following RF. Concurrently, a change in the annealing time at 450 °C leads to no significant variation in properties, whereas this change is noticeable at 500 °C. Increasing the PDA temperature to 550 °C is accompanied by the onset of static recrystallization processes, resulting in a different type of deformation diagram and a decrease in the strength characteristics of the alloy. It should be noted that the SMA TiNi rods, both following CT and RF with PDA, exhibit high plastic characteristics: subsequent to CT and RF, the elongation is 28%. Carrying out the PDA contributes to an additional increase in elongation. As shown in the work [15], the difference between the phase and dislocation yield strength ($\Delta\sigma$) indirectly indicates the ability of the alloy to recover shape. WRF, as well as WRF combined with PDA, leads to a twofold increase of this characteristic ($\Delta\sigma$) compared to CT. This indicates the positive effect of the applied TMP processes on both the mechanical and the functional characteristics of the alloy.

Table 1 Mechanical properties of SMA TiNi following WRF and PDA

TMP	σp, MPa	σmps, (δ = 6%) MPa	σy, MPa	Δσ, MPa	σB, MPa	δ, %
CT	100	150	430	330	700	28
WRF	275	515	935	660	1075	28
WRF + 450 °C, 0.5 h	80	125	835	755	947	38
WRF + 500 °C, 0.5 h	75	105	825	750	916	36
WRF + 450 °C, 1 h	75	125	825	750	942	48
WRF + 500 °C, 1 h	65	95	815	750	877	52
WRF + 550 °C, 1 h	115	100	775	660	820	58

Table 2 Functional characteristics of SMA TiNi following WRF and PDA

Treatment	t, %	i, %	e, %	r, %	f, %	SRR, %	A_S, °C	A_f, °C
RT	2.7	2.0	0.5	2.2	0	100	83	98
	7.4	6.0	1.4	3.5	2.5	58	90	107
WRF_{450}	2.7	0.3	2.4	0.3	0	100	45	55
	7.4	2.7	4.7	2.6	0.1	99	40	55
WRF_{450} + 450 °C, 0.5 h	3.0	2.2	0.8	2.2	0	100	61	74
	7.4	6.5	0.9	6.5	0	100	68	82
WRF_{450} + 500 °C, 0.5 h	2.6	2.2	0.4	2.2	0	100	55	68
	7.1	6.2	0.9	6.2	0	100	63	77
WRF_{450} + 450 °C, 1 h	2.7	2.2	0.5	2.2	0	100	60	78
	7.4	5.1	2.3	5.1	0	100	65	83
WRF_{450} + 500 °C, 1 h	2.6	2.2	0.4	2.2	0	100	50	65
	7.1	6.2	0.9	6.2	0	100	67	78
WRF_{450} + 550 °C, 1 h	2.7	2.0	0.7	2.0	0	100	70	78
	7.4	5.7	1.7	4.7	1.0	82	80	95

Results of functional tests

Table 2 shows the results of determining the fully reversible deformation and the temperature range of shape recovery during bending deformation.

The WRF is accompanied by an increase in internal stresses and a decrease in the TRSR compared to the defect-free state following CT. This behavior is typical of near-equiatomic titanium nickelide. An increase in the degree of induced strain from 2.7 to 7.4% for the samples following the WRF results in insignificant variations in the TRSR, which can be explained by large dislocation strain hardening. The combination of WRF and PDA, as well as RT, results in the formation of a less defective structure. An increase in the degree of induced bending strain leads to an increase in the TRSR by 15–25 °C. The PDA facilitates the static polygonization process, resulting in fewer defects in the crystal lattice. Moreover, the higher the PDA temperature and the longer the exposure time, the more pronounced this effect becomes: following the PDA at 550 °C for 1 h, the TRSR reaches the temperature values following the RT. When a strain of 7.1 to 7.4% is induced, no residual strain is detected following all the modes of WRF + PDA, except for PDA at 550 °C for 1 h, when the residual strain at the induced strain of 7.4% is 1.0%. This is due to the onset of the softening processes during annealing at this temperature. Therefore, it is impractical to use such a temperature and holding time if it is necessary to maintain high functional properties following WRF. It should be noted that the high values of elastic strain (4.7%) following inducing 7.4% bending strain following WRF indicate that the temperature range of forward

transformation is significantly shifted to lower temperatures, with the partial shape recovery occurring at room temperature due to the superelasticity effect. In general, the alloy is characterized by high values of maximum completely recoverable strain of 5.1–6.5% when 7.4% strain is induced following WRF combined with PDA.

Conclusion

This paper examines the impact of warm rotary forging (WRF) and post-deformation annealing at various temperatures and holding times, on the structure and mechanical properties of a near equiatomic alloy with shape memory based on titanium nickelide. On the basis of the results obtained, the following conclusions can be drawn:

1. Rotary forging at a temperature of 450 °C leads to the formation of a mixed submicrocrystalline structure in the TiNi alloy with the size of the structural elements in the range of 100–250 nm and a high density of dislocations. PDA at 450 °C has no noticeable effect on the increase in structural elements, indicating the stability of the formed structure.
2. WRF results in a significant increase in the ultimate tensile strength and yield strength of the alloy (1075 MPa to 935 MPa, respectively) compared to the reference treatment (700 MPa and 430 MPa, respectively). Following PDA at temperatures of 450 and 500 °C for 0.5–1 h, no sharp decrease in tensile strength and yield strength is observed, their values remaining above 900 and 800 MPa, respectively. PDA at 550 °C for 1 h is accompanied by a significant decrease in tensile strength and yield strength to 815 and 775 MPa, respectively.
3. The WRF of TiNi SMA leads to a noticeable decrease in the temperature of shape recovery due to strong strain hardening. The PDA facilitates the static polygonization process, resulting in fewer defects in the crystal lattice. Moreover, the higher the PDA temperature and the longer the exposure time, the more pronounced this effect becomes: following the PDA at 550 °C for 1 h, the TRSR reaches the temperature values following the RT.
4. The alloy is characterized by high values of maximum completely recoverable strain of 5.1–6.5% when 7.4% strain is induced following WRF combined with PDA.

Funding The study was carried out within the framework of project No. 23-19-00729 funded by the Russian Science Foundation, https://rscf.ru/project/23-19-00729/.

References

1. Brailovski V, Prokoshkin S, Terriault P, Trochu P (2003) Shape Memory Alloys: Fundamentals, Modeling, and Applications, Montreal, ETS. https://espace2.etsmtl.ca/id/eprint/3754
2. Gunther VE (2006) Titanium Nickelide. New Generation Medical Material [In Russian]. Tomsk, Izd. MIT
3. Resnina N, Rubanik V (2015) Shape memory alloys: Properties, technologies, opportunities. Trans. Tech. Publications, Praffikon
4. Jani JM, Leary M, Subic A, Gibson MA (2014) A review of shape memory alloy research, applications and opportunities. Mater Des 56:1078–1113 (1980–2015)
5. Sun Q, Matsui R, Takeda K, Pieczyska E (2017) Advances in Shape Memory Materials: In Commemoration of the Retirement of Professor Hisaaki Tobushi. Springer, vol 73. New York https://doi.org/10.1007/978-3-319-53306-3
6. Zareie S, Issa AS, Seethaler RJ, Zabihollah A (2020) Recent advances in the applications of shape memory alloys in civil infrastructures: a review. Structures 27:1535–1550 https://doi.org/10.1016/j.istruc.2020.05.058
7. Strittmatter J, Gümpel P, Hiefer M (2019) Intelligent materials in modern production—current trends for thermal shape memory alloys. Procedia Manuf 30:347–356
8. Zhu J, Zeng Q, Fu T (2019) An updated review on TiNi alloy for biomedical applications. Corros 37(6):539–552
9. Li HF, Nie FL, Zheng YF, Cheng Y, Wei SC, Valiev RZ (2019) Nanocrystalline Ti49. 2Ni50. 8 shape memory alloy as orthopedic implant material with better performance. J Mater Sci Technol 35(10):2156–2162

10. Dobrzański LA, Dobrzański LB, Dobrzańska-Danikiewicz AD, Dobrzańska J (2022) Nitinol type alloys general characteristics and applications in endodontics. Processes 10(1):101
11. Komarov V, Khmelevskaya I, Karelin R, Postnikov I, Korpala G, Kawalla R, Prahl U, Yusupov V, Prokoshkin S (2021) Deformation behavior, structure and properties of an Equiatomic ti–Ni shape memory alloy compressed in a wide temperature range. Trans Indian Inst Met 74:2419–2426. https://doi.org/10.1007/s12666-021-02355-x
12. Karelin R, Khmelevskaya I, Komarov V, Andreev V, Perkas M, Yusupov V, Prokoshkin S (2021) Effect of quasi-continuous Equal-Channel angular pressing on structure and properties of TiNi shape memory alloys. j Mater Eng Perform 30(4):3096–3106. https://doi.org/10.1007/s11665-021-05625-3
13. Karelin R, Komarov V, Khmelevskaya I, Andreev V, Yusupov V, Prokoshkin S (2023) Structure and properties of TiNi shape memory alloy after low-temperature ECAP in shells. Mater Sci Eng A 872:144960. https://doi.org/10.1016/j.msea.2023.144960
14. Komarov V, Khmelevskaya I, Karelin R, Prokoshkin S, Zaripova M, Isaenkova M, Korpala G, Kawalla R (2019) Effect of biaxial cyclic severe deformation on structure and properties of Ti-Ni alloys. J Alloys Compd 797:842–848. https://doi.org/10.1016/j.jallcom.2019.05.127
15. Prokoshkin SD, Brailovsky V, Korotitsky AV, Inaekyan KE, Glezer AM (2010) "Characteristics of structure formation of titanium nickelide during thermomechanical processing, including moderate to intense cold plastic deformation [In Russian], FMM 110(3):305–320

Authors and Affiliations

✉ V. A. Andreev
Andreev.icmateks@gmail.com

R. D. Karelin

V. S. Komarov

V. V. Cherkasov

N. A. Dormidontov

N. V. Laisheva

V. S. Yusupov

V. A. Andreev, R. D. Karelin, V. S. Komarov, V. V. Cherkasov, N. A. Dormidontov, N. V. Laisheva, V. S. Yusupov
A.A. Baikov Institute of Metallurgy and Material Science RAS, Moscow, Russian Federation

R. D. Karelin, V. S. Komarov, V. V. Cherkasov
University of Science and Technology MISIS, Moscow, Russian Federation